

4/p

UNPUBLISHED PRELIMINARY DATA



THEORY OF THE GEOMAGNETIC DAILY DISTURBANCE VARIATIONS

FACILITY FORM 802

N65-88714
(ACCESSION NUMBER)

(THRU)

41

(PAGES)

(CODE)

CR-74811
(NASA CR OR TMX OR AD NUMBER)

(CATEGORY)

by

J. A. Fejer

Southwest Center for Advanced Studies
P.O. Box 8478
Dallas 5, Texas

May 24, 1963



To be submitted to

JOURNAL OF GEOPHYSICAL RESEARCH

U.S. Government Agencies and
to U.S. Government Contractors only
and
U.S. Government Contractors only

Theory of the Geomagnetic Daily Disturbance Variations

X 63 14392

Code 2a

J. A. Fejer


Southwest Center for Advanced Studies
P.O. Box 8478, Dallas 5, Texas

ABSTRACT

over
14392

(The world-wide ionospheric current system) predicted by a previously described theory of the auroral electrojets (Fejer 1963) is computed. Tidal air motions are neglected at first, and the high latitude current system is assumed to be due entirely to the interaction of magnetospheric rotation with the belt of energetic protons which are trapped in the distorted geomagnetic field.) For a given geomagnetic distortion and trapped proton distribution, the computed current system strongly resembles Chapman's (1935) idealized Ds current system if sufficiently high E region electron concentrations independent of geographical position are assumed. As the assumed electron concentrations are decreased, however, the intensity of the computed current system is reduced, first in the auroral zone and then at all latitudes; at the same time, the phase of the current system is advanced in the polar cap and is retarded at low latitudes.

In view of this limitation of the current system by the available electron concentrations, (the large disturbance variations observed during an intense geomagnetic storm can only be explained by the present theory if in addition to an enhancement in the trapped proton density greatly enhanced E region electron concentrations are assumed, particularly in the



auroral zone. (Such enhanced electron concentrations are known to occur when blanketing sporadic E is observed.) The observed correlation between blanketing sporadic E and the strength of the electrojet current (Matsushita 1962) is thus predicted by the present theory.

The interaction of the tidal wind system with the belt of trapped protons is also considered. The resulting auroral electrojet currents oppose the Ds current system if the usually accepted pattern of upper atmospheric tidal winds (Maeda 1955) is assumed; the existence of a different wind pattern at high latitudes, at least during geomagnetic storms is a possibility that cannot altogether be excluded although it appears unlikely. If the majority of energetic particles in the radiation belt were electrons, then their interaction with the usually accepted tidal wind pattern would result in the correct phase for the Ds current system; satellite observations indicate, however, that the majority of the energetic particles are protons.

The present theory can also account for the generation of meridional static electric fields of the type that, according to a theory of McGill and Carleton (1963), cause mid-latitude red arcs.

1. Introduction

Ionospheric currents flowing at a height of about 100 km are believed to be the main cause of the disturbance daily variations Ds or S_D observed during geomagnetic storms. An idealized current system responsible for the mean Ds variation during 40 geomagnetic storms of moderate intensity has been proposed by Chapman (1935). A mean current

system for geomagnetic bays was derived by Silsbee and Vestine (1942).

Fukushima (1953) and more recently Fairfield (1963) have shown that at any one instant during a geomagnetic storm or an isolated geomagnetic bay, the current system may differ considerably from the mean current systems derived by Chapman (1935), Silsbee and Vestine (1942) and others. In general, the instantaneous current system is far more patchy than the averaged current systems derived from a long series of observations.

All these current systems show the presence of very strong easterly or westerly currents in the auroral zone; these are usually called auroral electrojets. The first theories of the auroral electrojets were essentially similar to the dynamo theory of the quiet day magnetic variations; a great local enhancement of the ionospheric conductivity, and possibly also of the wind velocities in the auroral zone, had to be assumed by these dynamo theories (Obayashi and Jacobs, 1957) to explain the Ds current system. An additional difficulty arose in connection with the phase of the Ds current system predicted by the dynamo theories (Matsushita 1953, Maeda 1957); a wind system at high latitudes, whose phase is opposed to the phase of the wind system responsible for the Sq variations, had to be assumed.

Kern (1961), Fejer (1961), and Chamberlain (1961) have independently suggested that charge separation caused by the adiabatic motion of energetic trapped particles could lead to the auroral electrojet currents. Currents produced by this type of charged separation alone are, however, necessarily temporary in character.

In a subsequent paper (hereafter referred to as I) Fejer (1963) suggested that the interaction of magnetospheric motions with the belt of

energetic trapped protons observed by Explorer XII (Davis and Williamson 1962) could lead to steady auroral electrojet currents without a local enhancement of ionospheric conductivity or wind velocity at auroral latitudes. The suggestions put forward in I are considered in this paper in a more quantitative manner by the computation of world-wide current systems. The main purpose of the calculations is to examine the reaction of the electric fields necessary to drive the current system in the ionosphere, on the original magnetospheric motions that were assumed to cause the current system. This effect was ignored in I.

2. The Current Generating Mechanisms Proposed in (I)

2.1 The interaction of magnetospheric rotation with energetic protons trapped in a distorted geomagnetic field

This first mechanism is illustrated schematically by Fig. 1, which shows a cross section of the belt of trapped particles in the equatorial plane. It is assumed that the energetic protons detected by Explorer XII (Davis and Williamson 1962) represent the majority of energetic trapped particles present. The belt is thus assumed to have a positive space charge which must be at all times approximately compensated by the space charge of the low energy plasma. Both the low energy plasma and the energetic trapped particles partake in any magnetospheric drifts caused by the presence of electric fields; the energetic particles also partake in an additional drift caused by the inhomogeneity of the magnetic field. The latter drift is much faster for the energetic particles than the former and causes them to drift around the earth in a relatively short time. The equatorial crossing points of the guiding center of a particle

trapped in an undistorted dipole magnetic field would lie on a circle concentric with the dipole axis. This circle would be only slightly modified by the presence of magnetospheric electric fields; the modification will be neglected in the present paper.

When the geomagnetic field is distorted by the solar wind, the path of the equatorial crossing point of an energetic trapped particle is also distorted; the crossing points lie closer to the earth on the night side than on the day side. This is illustrated schematically by Fig. 1, where the shaded region represents the equatorial crossing points of the proton belt in the distorted geomagnetic field. Fig. 1 also shows the path of flow of the low energy plasma on the assumption that the only magnetospheric motion is that due to the earth's rotation. As a field line approaches the subsolar position, it reaches its maximum compression; thus the rotating low energy plasma is closest to the earth in the subsolar direction and is furthest on the night side (in the antisolar direction). The net result is that the low energy plasma tries to stream across the high energy proton belt, inward on the morning side and outward on the evening side, as seen from Fig. 1. Such a motion tends to upset the balance of space charge since the excess negative space charge of the low energy particles, that compensates for the positive space charge of the energetic protons, streams inward or outward. Charge neutrality is nearly restored by currents along the highly conducting field lines which link the magnetosphere to the ionosphere and by ionospheric currents. The ionospheric currents are driven by electric polarization fields due to the residual space charge. These polarization

fields also produce drift motions in the magnetosphere in addition to that of the earth's rotation. If the ionospheric conductivity is sufficiently high, these secondary motions may be neglected as they were in I. In reality, the ionospheric conductivity is not infinitely high and the study of the reaction of the electric fields, required to drive the ionospheric currents, on the original motions of the magnetosphere is the main purpose of the present paper.

2.2 The interaction of the tidal wind system with the belt of energetic trapped protons

A second current generating mechanism, also proposed in I, made use of the magnetospheric motions associated with the tidal wind system and with the dynamo current system caused by these tidal winds. These magnetospheric motions interact with the belt of trapped protons. The currents caused by this interaction are additional to the ordinary dynamo current system. It will be shown in this paper that the additional current system is essentially similar to the current system produced by the interaction of magnetospheric rotation with the proton belt in the distorted geomagnetic field (the first mechanism). The current systems caused by these two mechanisms are determined by the same type of differential equation and are both caused by the streaming of low energy plasma across the belt of energetic trapped charged particles. The distortion of the geomagnetic field is essential to the first, but not to the second mechanism.

3. Method of Computation of the Ionospheric Current System

The computations described in this section resemble the computations

of ionospheric current systems caused by tidal motions. The simplifying assumptions made are essentially similar to those made in a paper (hereafter referred to as II) by Fejer (1953). The earth's magnetic axis is assumed to coincide with the axis of rotation and the direction of the solar wind is assumed to be perpendicular to both axes. The atmospheric wind system, which is required only for the second mechanism, is taken to be symmetrical with respect to the equator. In the dynamo theory, this results in the restriction of the current system to a thin current-carrying shell between approximately 90 and 150 km. Although in the present calculations this is not true near the auroral zone, the expressions for the height-integrated conductivities given in II, where the vertical current density was assumed to vanish, are used. The error caused in this manner may be shown to be very small.

In the present calculations the tidal wind velocity components are taken to vary harmonically with local time (longitude), with a period of 24 hours, and the height-integrated conductivity is taken to be independent of the latitude and the longitude. The computer program provides, however, for the possible presence of tidal winds with periods of $24/n$ hours, where n is an integer, and for a possible variation of conductivity with latitude.

Apart from the tidal winds, the atmosphere below, say, 150 km is taken to rotate with the earth and is thus stationary, when considered from a system rotating with the earth. All equations of this paper refer to such a rotating coordinate system.

The lines of force in the magnetosphere are also very nearly lines of equal potential because the effective conductivity parallel to the

magnetic field is very high. The motion of low energy plasma perpendicular to the magnetic field is governed by the polarization electric field which is very nearly perpendicular to the field lines. These motions of the low energy plasma take place in such a manner that the particles which at one time occupy a certain tube of force, continue at all later times to occupy a tube of force of equal flux content. The motions appear as interchanges of tubes of force and could be fully described by the motion of the feet of the lines of force on the ionospheric shell. Let Q be half the space charge of the low energy plasma filling a tube of force which carves out an area of 1 cm^2 from the ionospheric shell at each of its feet and let \underline{v}_D be the velocity of the foot of the line of force on the ionospheric shell. Then the linear current density, caused by the motion of the low energy magnetospheric plasma, projected along the lines of force to the ionospheric shell, may be expressed as $Q\underline{v}_D$. Here \underline{v}_D is caused only by the presence of electric fields seen from a rotating frame of reference and, therefore, does not include the earth's rotation. The space charge Q approximately compensates at all times the space charge $-Q$ of the energetic trapped particles. In a stationary state, with the present assumptions of symmetry, the space charge $-Q$ of the energetic particles would be fixed in space if regarded from a non-rotating coordinate system; in a rotating system, after projection to the ionospheric shell along the lines of force, the space charge $-Q$ appears to move at an apparent velocity $-\underline{v}_R$, where \underline{v}_R is the velocity of rotation of the earth's ionospheric shell (where the neutral atmosphere is assumed to rotate with the earth). The apparent height-integrated current density projected

to the ionospheric shell, caused by the presence of the belt of trapped energetic particles, is thus $(-Q) \cdot (-\underline{v}_R) = Q\underline{v}_R$, as observed from a rotating coordinate system.

In addition to these magnetospheric currents across the field lines, which may be expressed as height-integrated current densities $Q\underline{v}_D$ and $Q\underline{v}_R$ after projection to the ionosphere along the lines of force, there are also ionospheric currents caused by the polarization electric field \underline{E}_p and, if the second mechanism is operative, also by the dynamo electric field \underline{E}_i where the terminology of II is used. If the height-integrated ionospheric current density is denoted by \underline{j} , then the conservation of charge demands that no overall accumulation of charge should take place in a tube of force. The height-integrated current densities (projected to the ionospheric shell) $Q\underline{v}_D$, $Q\underline{v}_R$ and \underline{j} must therefore satisfy the equation

$$\text{div} (\underline{j} + Q\underline{v}_R + Q\underline{v}_D) = 0 \quad (1)$$

over the ionospheric shell. This equation is of general validity and may be applied to both mechanisms, or in the special case $Q = 0$ to the tidal dynamo theory.

Assumptions about the space charge density $-Q$ of the energetic particles must be made in order to solve equation (1). In an undistorted geomagnetic field and with the present assumptions of symmetry, the value of Q would depend only on the colatitude θ . In a geomagnetic field distorted by the solar wind, Q also depends on the longitude (local time). This asymmetry arises because the trapped energetic particles, the

majority of which are taken to be protons, are trapped on field lines whose feet are at lower latitudes on the day side than on the night side. This apparent diurnal latitude shift of the proton belt is regarded here as small, independent of latitude and a harmonic function of longitude (local time) with a period of 360° (24 hours). This is undoubtedly a rather crude representation of the true proton belt, but it can lead to useful results. It is convenient to write $Q = Q_1(\theta) + Q_2(\theta, \varphi)$ where θ is the colatitude and where Q_2 is much smaller than Q_1 and is a harmonic function of φ , the longitude angle measured eastward from a reference longitude. It is assumed that $Q_1(\theta)$ is given by the triangular function of Fig. 2; the functions derived in I, based on the results of Davis and Williamson (1962), are shown by the solid curve (in which a low energy cut-off at 80 keV is assumed for the proton spectrum) and the dashed curve (for which the assumed cut-off energy is 60 keV). If the latitudinal displacement of the eccentric proton belt is $\Delta\theta \sin(\varphi - \varphi_0)$, then the number of protons between φ and $\varphi + d\varphi$ and between θ and $\theta + d\theta$ changes from $Q_1(\theta) 2\pi R^2 \sin\theta d\theta d\varphi$ to $Q_1[\theta + \Delta\theta \sin(\varphi - \varphi_0)] 2\pi R^2 \sin[\theta + \Delta\theta \sin(\varphi - \varphi_0)] d\theta d\varphi$. The amount of the change is thus $[(\partial Q_1 / \partial \theta) \sin\theta + Q_1 \cos\theta] 2\pi R^2 \sin(\varphi - \varphi_0) \Delta\theta d\theta d\varphi = Q_2(\theta, \varphi) 2\pi R^2 \sin\theta d\theta d\varphi$, where R is the radius of the ionospheric shell. Solving for Q_2 results in

$$Q_2(\theta, \varphi) = \left(\frac{\partial Q_1}{\partial \theta} + Q_1 \cot\theta \right) \sin(\varphi - \varphi_0) \Delta\theta = Q_{20}(\theta) \sin(\varphi - \varphi_0) \quad (2)$$

where $Q_{20}(\theta)$ is defined by equation (2).

The south and east component of the height-integrated ionospheric current density are given by

$$j_x = \sigma_{xx} E_x + \sigma_{xy} E_y \quad (3)$$

$$j_y = -\sigma_{xy} E_x + \sigma_{yy} E_y \quad (4)$$

where σ_{xx} , σ_{xy} , σ_{yy} are the height-integrated conductivities defined in II and where the electric field $\underline{E} = \underline{E}_i + \underline{E}_p$ is the sum of dynamo electric field \underline{E}_i resulting from the atmospheric wind system (seen from the rotating earth) and of the static polarization field $\underline{E}_p = -\text{grad } \Psi$ where Ψ is the electrostatic potential. The components of the velocity \underline{v}_R are

$$v_{Rx} = 0, \quad v_{Ry} = \Omega R \sin\theta \quad (5)$$

where Ω is the angular velocity of the earth. The drift velocity \underline{v}_D of the foot of a tube of force has the components (cf., Equations 2 and 3 of I)

$$v_{Dx} = -E_{py}/B \sin X, \quad v_{Dy} = E_{px}/B \sin X \quad (6)$$

where X is the angle of inclination of the geomagnetic induction \underline{B} . The differential equation (1) may now be written in the form

$$\frac{\partial}{\partial \theta} [\sin\theta (j_x + Qv_{Rx} + Qv_{Dx})] + \frac{\partial}{\partial \phi} (j_y + Qv_{Ry} + Qv_{Dy}) = 0 \quad (7)$$

where $j_x j_y$, v_{Rx} , v_{Ry} , v_{Dx} , and v_{Dy} are given by equations (3), (4), (5), and (6). The conductivities σ_{xx} , σ_{xy} , and σ_{yy} were assumed to be given by the equations (cf., equation 24 of II)

$$\sigma_{xx} = L^{-1} (\int \sigma_1 dh) (\int \sigma_0 dh) \quad (8)$$

$$\sigma_{xy} = - L^{-1} (\int \sigma_2 dh) (\int \sigma_0 dh) \sin X \quad (9)$$

$$\sigma_{yy} = L^{-1} \left[(\int \sigma_1 dh) (\int \sigma_0 dh) \sin^2 X + (\int \sigma_1 dh) (\int \sigma_3 dh) \cos^2 X \right] \quad (10)$$

where L is given by

$$L = (\int \sigma_1 dh) \cos^2 X + (\int \sigma_0 dh) \sin^2 X . \quad (11)$$

Values of $\int \sigma_0 dh$, $\int \sigma_1 dh$, $\int \sigma_2 dh$, and $\int \sigma_3 dh$ independent of the colatitude are assumed in the computations to be described here. A purely diurnal variation of all the quantities is assumed. Thus, the potential Ψ is taken as

$$\Psi = - R(\Psi_a \sin \varphi + \Psi_b \cos \varphi) . \quad (12)$$

The polarization field is then given by

$$E_{px} = \frac{\partial \Psi_a}{\partial \theta} \sin \varphi + \frac{\partial \Psi_b}{\partial \theta} \cos \varphi \quad (13)$$

$$E_{py} = - \frac{\Psi_b}{\sin \theta} \sin \varphi + \frac{\Psi_a}{\sin \theta} \cos \varphi . \quad (14)$$

The tidal dynamo field is assumed to be given by

$$E_{ix} = E_a(\theta) \sin \varphi \quad (15)$$

$$E_{iy} = E_b(\theta) \cos \varphi \quad (16)$$

and the components of the tidal wind system with periods that are submultiples of 24 hours, are thus ignored. These equations determine the position of the reference meridian with respect to the tidal wind system. Equations (2), (3), (4), (5)', (6), (7), (13), (14), (15), and (16) may be combined to yield (if $Q_{20} \ll Q_1$ is assumed and the earth's magnetic field is taken as a dipole field whose induction at ionospheric heights over the magnetic pole is B_0) the equations

$$\frac{\partial^2 \psi_a}{\partial \theta^2} + \alpha \frac{\partial \psi_a}{\partial \theta} - \beta \psi_a - \gamma \psi_b - \delta = 0 \quad (17)$$

$$\frac{\partial^2 \psi_b}{\partial \theta^2} + \alpha \frac{\partial \psi_b}{\partial \theta} - \beta \psi_b + \gamma \psi_a - \xi = 0 \quad (18)$$

where

$$\alpha = (\sigma_{xx} \sin \theta)^{-1} \frac{\partial}{\partial \theta} (\sigma_{xx} \sin \theta) \quad (19)$$

$$\beta = \sigma_{yy} / \sigma_{xx} \sin^2 \theta \quad (20)$$

$$\gamma = (\sigma_{xx} \sin \theta)^{-1} \frac{\partial}{\partial \theta} \left(\sigma_{xy} - \frac{Q_1}{B_0 \cos \theta} \right) \quad (21)$$

$$\delta = (\sigma_{xx} \sin \theta)^{-1} \left[\frac{\partial}{\partial \theta} (E_a \sigma_{xx} \sin \theta) - E_b \sigma_{yy} + Q_{20} R \Omega \sin \theta \sin \varphi_0 \right] \quad (22)$$

$$\xi = (\sigma_{xx} \sin \theta)^{-1} \left[\frac{\partial}{\partial \theta} (E_b \sigma_{xy} \sin \theta) - E_a \sigma_{xy} + Q_{20} R \Omega \sin \theta \cos \varphi_0 \right] \quad (23)$$

These two simultaneous linear second order differential equations determine ψ_a and ψ_b , and thus indirectly the polarization field \underline{E}_p (cf., eq. 13 and 14) and the current density \underline{j} (cf., eq. 3, 4, 8, 9, 10, 11). After the introduction of two new variables $u_a = \partial \psi_a / \partial \theta$ and $u_b = \partial \psi_b / \partial \theta$, the

four first order simultaneous differential equations resulting from equations (17) and (18) were solved numerically by the Runge-Kutta method. Two particular solutions of the reduced equations and one particular solution of the complete equations were superimposed to satisfy the boundary conditions near the pole as outlined in II; the solutions were carried to within 0.5° of the pole.

If Q_1 and Q_{20} are set equal to zero in equations (17 - 23), then they become almost equivalent to equations (17) and (18) of II although the present equations apply to diurnal variations, whereas the equations in II applied to semidiurnal variations. It has already been mentioned that the program was in fact written for a tidal wind period of $24/n$ hours. The program could thus be checked against the numerical solution obtained in II.

Equations (17 - 23) may be applied to either of the two mechanisms discussed in the previous section. In the first mechanism the interaction of magnetospheric rotation with the belt of protons trapped in a disturbed geomagnetic field was considered; the corresponding solution of equations (17 - 23) is obtained by setting $E_a = E_b = 0$. The solution is clearly proportional to $\Delta\theta$, i.e., to the distortion of the geomagnetic field. The dependence of the solution on the conductivities and on Q_1 , the equivalent surface charge density of the proton belt, is more complex as will be shown in the next section.

The second mechanism is based on the interaction of tidal motions with the trapped proton belt; the corresponding solution of equations (17 - 23) is obtained by setting $Q_{20} = 0$. It is particularly instructive

to find the differential equations for the difference between the solutions in the absence and in the presence of the trapped protons.

If Ψ_a , Ψ_b are the solutions in the absence of the trapped protons and $\Psi_a + \Delta\Psi_a$, $\Psi_b + \Delta\Psi_b$ are the solutions in the presence of the trapped protons, then it may be easily shown that $\Delta\Psi_a$ and $\Delta\Psi_b$ satisfy differential equations which may be obtained from equations (17 - 23) if $\Delta\Psi_a$ and $\Delta\Psi_b$ are substituted for Ψ_a and Ψ_b , E_a and E_b are set equal to zero and the expressions

$$Q_{20} \sin \varphi_o = \frac{-\Psi_b(\theta)}{R\Omega \sin \theta} \frac{\partial}{\partial \theta} \left(\frac{Q_1}{B_o \cos \theta} \right) \quad (24)$$

$$Q_{20} \cos \varphi_o = \frac{\Psi_a(\theta)}{R\Omega \sin \theta} \frac{\partial}{\partial \theta} \left(\frac{Q_1}{B_o \cos \theta} \right) \quad (25)$$

are used to define Q_{20} and φ_o . The definition of Q_{20} by (24) and (25) resembles the definition of Q_{20} by (2) in terms of the displacement of the proton belt, due to geomagnetic distortion; in both cases Q_{20} is roughly proportional to $\partial Q_1 / \partial \theta$ since Q_1 is a rapidly varying function of the latitude. The two definitions are roughly identical if $\Omega R \Delta \theta = (\Psi_a^2 + \Psi_b^2)^{1/2} / B_o \sin \theta \cos \theta$, or if the plasma streaming velocities across the proton belt are the same. This shows that the perturbation of the tidal dynamo current system by the belt of trapped protons produces an additional current system that is essentially similar to the current system due to the interaction of magnetospheric rotation with the belt of protons trapped in a distorted magnetic field, although it may not agree with it in phase.

In view of the similarity of the two current systems only the one due to geomagnetic distortion by the solar wind will be computed in the

following section, although a discussion of both current generating mechanisms will follow.

4. Computations of Ionospheric Current Systems

The following assumptions are common to all computations discussed in the present section: $E_a = E_b = 0$ (no tidal motions), $\Delta\theta = 7^\circ$, $\int \sigma_2 dh / \int \sigma_1 dh = 3.5$, $\int \sigma_3 dh / \int \sigma_1 dh = 30$, $\int \sigma_o dh / \int \sigma_1 dh = 100$. The value $\Delta\theta = 7^\circ$ corresponds to a fairly large geomagnetic distortion and a maximum plasma streaming velocity of $\Omega R \Delta\theta = 58$ m/sec across the proton belt. The current system is proportional to $\Delta\theta$ and thus the results of the computations can easily be modified to apply to any value of $\Delta\theta$. The assumed ratios of the height-integrated conductivities are identical to those used in II. The first two of these ratios could have values considerably smaller than those assumed above, particularly at night in the absence of sporadic E ionization when the F region makes a relatively large contribution to $\int \sigma_1 dh$ but not to $\int \sigma_2 dh$; on the other hand, in the presence of very strong sporadic E ionization the ratios may well have values higher than the assumed ones.

Four computations have been carried out corresponding to $\int \sigma_2 dh = 46$, 14, 4.6, and 0.46 m.k.s. units (mhos). These solutions remain valid if $\int \sigma_2 dh$ (and the other height-integrated conductivities), the computed current density, and the assumed distribution of Q (cf., Fig. 2) are all multiplied by a constant factor.

The computed current systems are shown by Figures 3a - 3d. The electric fields driving the currents may be derived from Figures 4a - 4c,

which show lines of equal potential for the first three values of $\int \sigma_2 dh$. The Hall current flows in the direction of the lines of equipotential so that Figures 4a - 4c indicate, in a sense, the flow lines of the Hall current, which does not differ greatly from the total ionospheric current under the present assumptions, except in the vicinity of the geomagnetic equator. The potential difference ΔV between neighboring lines is indicated on each of the Figures 4a - 4c; Figures 4a and 4b are drawn somewhat inaccurately in the auroral zone where some of the lines would otherwise merge with each other.

Figure 3a shows the amplitude and phase of the ionospheric current for a height-integrated conductivity $\int \sigma_2 dh = 46$ mhos, which is about twice as high as the mid-day conductivity at moderate latitudes (Chapman 1956). The current system represented by Fig. 3a closely resembles Chapman's (1935) idealized Ds current system. The east-west currents in the auroral zone are exactly out of phase with those at higher or lower latitudes. In the auroral zone, the change from a current towards the east to a current towards the west is seen to occur at almost exactly midnight. The amplitude of the east-west current density has a very pronounced maximum in the auroral zone and a very much weaker maximum at the equator. The auroral zone maximum of about 63 amps/km corresponds to a change in the horizontal component of the magnetic field of about 80γ if the earth is taken to be a perfect conductor and the magnetic field change is taken to be caused by a uniform ionospheric current density and an earth current density of equal magnitude and opposite direction.

Figure 3b shows that the maximum current density in the auroral zone decreases very little as the conductivity is decreased to $\int \sigma_2 dh = 14$ mhos. There is, however, a change in the phase of the currents north and south of the auroral zone; the phase of the currents is advanced in the polar cap and is retarded at lower latitudes by about two hours. The change from east to west in the direction of current flow still occurs nearly at midnight in the auroral zone.

Figure 3c shows that as the conductivity is decreased further to $\int \sigma_2 dh = 4.6$ mhos, the maximum current density in the auroral zone is reduced considerably to about 22 amps/km, corresponding to a magnetic field change of only 28 $\%$. The current density in the polar cap and at low latitudes is not yet significantly changed by the reduced conductivity. As the conductivity is further reduced, however, to $\int \sigma_2 dh = 0.46$ mhos, the current density is greatly reduced at all latitudes as shown by Fig. 3d. It should be pointed out here that when the value of the height-integrated Hall conductivity reaches such low values, the ratio $\int \sigma_2 dh / \int \sigma_1 dh$ is probably much lower than the value of 3.5 assumed in the computations and may even be smaller than unity. No computations were carried out for such low ratios of $\int \sigma_2 dh / \int \sigma_1 dh$.

Figure 4a shows a remarkable similarity of the Hall current system to Chapman's (1935) idealized Ds current system; the similarity would be even greater if the total currents rather than the Hall currents were displayed. The electric fields are relatively weak; they would be vanishingly small for an infinitely high conductivity. It is interesting to note that the two lines of equipotential (or Hall current flow)

nearest to the pole (not the line through the pole) have an entirely different shape from the other lines; a similar pair of current flow lines is shown by the Ds current system given by Fig. 3c of Obayashi and Jacobs (1957) (originally due to Vestine et al 1947). As the conductivity is reduced, more lines of equipotential assume the peculiar shape of the above two lines; at the same time the current system is rotated clockwise in the polar cap and anticlockwise at low latitudes as shown by Fig. 4b. A further reduction of conductivity results in the lines of equipotential of Fig. 4c, in which the clockwise and counterclockwise rotation of the polar cap and low latitude current systems approaches 90° . It should be noted that the electric fields are largest when the conductivity is lowest, i.e., on Fig. 4c.

5. Required and Available Ionospheric Conductivities

The most important single result of the present computations is the limitation of the proposed mechanism by the available ionospheric conductivity. The computations were based on the quiet time proton belt and show (cf., Fig. 3b) that at quiet times, a height-integrated Hall conductivity of 14 mhos can result in horizontal field changes of about 70γ . In the summer, the ionospheric conductivity due to solar ultraviolet radiation is not far short of this value and is thus sufficient to explain the Ds-like current observed during quiet days (Fairfield 1963). It is to be emphasized that the assumed values of Q and $\Delta\theta$ were to some extent arbitrary and much larger values of Q may occur even at quiet times.

The results of the computations make it clear that much larger values of both Q and $\int \sigma_2 dh$ than those used in the calculation leading to Fig. 3b, would be required to account for the magnetic variations observed during storms. If Fig. 3c were reinterpreted as a ten times more intense current system caused by ten times larger values of Q than those indicated in Fig. 2 and a height-integrated Hall conductivity of $\int \sigma_2 dh = 46$ mhos, then such a current system would explain the large magnetic variations of several hundred gammas observed during magnetic storms. Such a high conductivity would probably be present during sporadic E conditions. Under such conditions the conductivity would probably be higher in the auroral zone, where the limitation of the current by conductivity is most severe, than in the polar cap.

The results of the present computations also explain the observed correlation between blanketing sporadic E and magnetic disturbances (Matsushita 1962); both are (at least partly) manifestations of enhanced ionospheric electron concentrations at heights of about 100-140 km.

It should be pointed out here that the current generating mechanism of the present paper tends to act as a source of constant current, as shown by Figures 3a and 3b, while the ionospheric conductivity is sufficiently high. The limitation of the current system is caused by the reaction of the electric fields, that drive the ionospheric currents, on the motions of the magnetosphere. Since the driving electric fields are primarily meridional, they cause mainly azimuthal magnetospheric motions that, in the first approximation, do not react back on the original meridional magnetospheric motions responsible for the current

system. The driving electric fields are not, however, exactly meridional and therefore some feedback does occur and eventually limits the current system, as shown by the results of this paper. It should be emphasized that the present calculations only indicate the limitation of the total electrojet current by conductivity; the height-integrated or linear current densities could be considerably greater than those calculated in this paper if the latitude range of the trapped protons were smaller than the 16° used in the computations, or if an enhancement of Q occurred over a very narrow latitude range.

6. Motions in Radar Echoes from Aurora and Ionospheric Conductivity

In addition to the sporadic E traces on ionograms, there is indirect evidence to indicate that the night-time Hall conductivity of the E region is considerably higher near the auroral zone, at least when radio aurora is observed, than the conductivity due to a decaying E layer which was produced by solar photons during the day. Lyon and Kavadas (1958) have shown that the direction of motion (east or west) of auroral radar echoes is strongly correlated with the direction of the auroral electrojet. If the mean values of the velocity are compared to mean values of the magnetic disturbance, then a velocity of 15 km/min or 250 m/sec corresponds to a horizontal magnetic disturbance of 150 γ (cf., Fig. 6 of Lyon and Kavadas). If the velocity of motion of auroral echoes is interpreted as a plasma drift velocity in the presence of combined electric and magnetic fields, a velocity of 250 m/sec corresponds to an electric field of 14 volts/km. A magnetic disturbance of 150 γ , if interpreted as a result of a uniform ionospheric current sheet and a

corresponding earth current sheet of equal intensity, corresponds to a height-integrated ionospheric current density of 120 amps/km. The corresponding height-integrated Hall conductivity σ_{xy} is therefore $120/14 = 8.6$ mhos, a value that would be more characteristic of midday than of nighttime conditions at auroral latitudes if solar photons were the only cause of the ionization. Moreover, Lyon and Kavadas (1958) show that individual values of the velocity and the magnetic field are not at all well correlated in magnitude although they are almost perfectly correlated in sign (direction). In this interpretation, lack of correlation in magnitude will have to be explained by changes in ionospheric conductivity. The lowest observed conductivity would be represented by a combination of a velocity of about 30 km/min with a magnetic disturbance of about 200 γ on the scatter plot given by Lyon and Kavadas (their Fig. 7); a height-integrated conductivity $\sigma_{xy} \sim \int \sigma_2 dh \sim 5.7$ mhos is obtained. The highest value of the conductivity obtained from the scatter plot would be infinity if the large number of points with zero velocity and high magnetic disturbance were used. Even if the points with zero velocity are ignored, a combination of a velocity of 7 km/min with a disturbance of 500 γ leads to a maximum height-integrated conductivity of 62 mhos, a value far higher than the height-integrated midday conductivity at moderate latitudes but not impossibly high for severe sporadic E conditions.

7. Diurnally Recurring Events

The present assumption, made for its convenience in computations, of an asymmetric proton belt in a dipole magnetic field is highly artificial. The orbits of trapped particles in a magnetic field distorted by the solar wind have been studied by Hones (1963) on a somewhat more realistic basis. His results show that a belt of protons with relatively high equatorial pitch angles must be concentrated over a more narrow range of lower latitudes (projected to the earth along field lines) on the night-side than on the day-side; this would lead to a more narrow electrojet current at a lower latitude on the night-side than on the day-side. An observing station of a given magnetic latitude will thus change its position in the north-south direction with respect to the electrojet current as it rotates underneath it. If a current density enhancement within the electrojet were to occur over a very narrow range of latitudes, then the observed magnetic field of the enhanced current would be greatest when the observing station passed under it. This would occur twice a day at two separate local times, different for different stations, and perhaps the observed daily recurrences of certain features of magnetic records for several days (Chapman and Bartels 1940) may be explained in this manner.

8. The Second Mechanism

It was tacitly assumed in the preceding discussion that the distortion of the geomagnetic field by the solar wind and the resulting streaming of exospheric low energy plasma across the proton belt (the first mechanism),

illustrated by Fig. 1, causes the current system responsible for magnetic disturbances. A streaming of exospheric low energy plasma across a belt of high energy trapped protons can, however, also be caused by any exospheric electrostatic polarization field that has a component parallel to the shell of trapped protons (the second mechanism). The polarization field associated with the tidal dynamo currents (Martyn 1947) should therefore also lead to a current system similar to that caused by the mechanism of Fig. 1, but of the opposite phase if the generally accepted phase of the tidal polarization field (Maeda 1955) is assumed. It thus appears that the tidal polarization fields cannot cause the observed disturbance variations unless electrons predominate among the high energy particles. Satellite observations indicate, however, that the majority of high energy particles are protons. The unlikely possibility of an entirely separate high altitude wind system of the required phase at high latitudes cannot, however, be altogether disregarded. An experimental determination of wind velocities in the 100-140 km range in the auroral zone would be of considerable interest in this connection.

9. The Dynamo Theory of Auroral Electrojets

If the possibility of a high altitude wind system whose phase at auroral latitudes differs from the usually accepted phase of the tidal wind system (Maeda 1955) is admitted, then the Ds current system and the auroral electrojets could, in principle, be produced by dynamo action combined with an enhancement of ionospheric conductivity in the auroral zone. Maeda (1957) already discussed such a mechanism and derived the wind system required to produce the observed Ds variations on the

assumption of enhanced ionospheric auroral zone conductivities consistent with sporadic E observations. The wind velocities obtained by him were very high (200-400 m/sec), and the wind patterns were rather complicated and very different from the tidal pattern.

More recently Swift (1963a, 1963b) again considered the dynamo mechanism as a cause of auroral electrojets. In his first paper (Swift 1963a) he considered a one-dimensional mechanism in which a uniform wind was blowing across a horizontal strip of enhanced conductivity; the conductivity was taken to depend only on one horizontal coordinate. (There is an inconsistency in this first paper of Swift because he applies the one-dimensional result to a model in which the conductivity also depends on the height, and in this way he greatly overestimates the electrojet current resulting from his model.)

In a second paper Swift (1963b) considers a more realistic two-dimensional mechanism in which the conductivity is taken to depend on both horizontal coordinates (but is still independent of the height). He considers the interaction of a uniform wind with a narrow ring of enhanced conductivity (such as would exist in the auroral zone) and shows that the resulting current system is very different from the Ds current system derived from magnetic observations. The computed current density almost vanishes inside the ring, although the observations indicate a high Ds current density over the polar cap; Swift's work thus confirms Maeda's (1957) conclusion that a purely dynamo theory of the Ds current system requires a rather complicated wind system which is unlikely to exist.

10. Mid-latitude Red Arcs

Another application of the theory outlined in I and in this paper has been suggested to the author by L. R. Megill and N. P. Carleton. Calculations by Megill and Carleton (1963) suggest that mid-latitude red arcs and the high altitude red portion of type-A aurora are caused by static meridional electric polarization fields very similar to those that are produced by the mechanisms of I and the present paper if the existence of a belt of trapped particles over a narrow range of magnetic latitudes above the red arc is assumed. At mid-latitudes the interaction of these trapped particles with magnetospheric motions of tidal origin is probably more important than their interaction with magnetospheric rotation in a distorted geomagnetic field. Since the interaction mechanism resembles a constant current generator, the generated electrostatic fields will be most intense at night when the ionospheric conductivity is low. The feedback of the electric field on the original magnetospheric motions is believed to be relatively small on account of the small latitude range of the arc.

11. Conclusions

It has been shown that the interaction of trapped energetic protons with magnetospheric rotation in a geomagnetic field distorted by the solar wind could cause the observed Ds disturbance variations of the magnetic field. The quiet day Ds-type variations (Fairfield 1963) are reasonably well explained if a belt of energetic protons derived from Explorer XII observations (Davis and Williamson 1962) is assumed; the E region ionization produced by solar ultraviolet radiation provides a sufficiently

conducting path for the currents produced, at least in daytime. The large Ds variations observed during magnetic storms can, on the other hand, only be explained if in addition to the enhancement in the number of trapped protons a large enhancement in ionospheric conductivity, to values considerably greater than those characteristic of moderate latitudes at midday, is postulated, particularly at night. Such an enhancement could occur during sporadic E conditions. It is suggested that radar observations of auroral motions (Lyon and Kavadas 1958) could be interpreted as evidence for the existence of such high conductivities at times when auroral radar reflections are observed.

ACKNOWLEDGMENTS

Mr. L. B. Wadel constructed the program for the problem and performed the computations. Thanks are due Drs. L. R. Megill, N. P. Carleton, W. B. Hanson, T. N. L. Patterson, and F. S. Johnson for helpful discussions.

This research was supported by the National Aeronautics and Space Administration under Grant NsG-269-62.

REFERENCES

- Chamberlain, J. W., Theory of auroral bombardment, *Astrophys. J.*,
134, 401-429, 1961.
- Chapman, S., The electric current-systems of magnetic storms, *Terr. Mag.*,
40, 349-370, 1935.
- Chapman, S., The electrical conductivity of the ionosphere: a review,
Nuovo cimento, 4 Series X, Supplement, 1385-1412, 1956.
- Chapman, S. and J. Bartels, *Geomagnetism*, Oxford University Press, 1940.
- Davis, L. R. and J. M. Williamson, Low-energy trapped protons, in *Proc.*
Intern. Space Sci. Symp., 3rd, Washington, 1962.
- Fairfield, D. H., Ionosphere current patterns in high latitudes,
Scientific Report No. 171, Ionosphere Research Laboratory, Pennsylvania
State University, 1962.
- Fejer, J. A., Semidiurnal currents and electron drifts in the ionosphere,
J. Atmospheric Terrest. Phys., 4, 184-203, 1953.
- Fejer, J. A., The effects of energetic trapped particles on magnetospheric
motions and ionospheric currents, *Can. J. Phys.*, 39, 1409-1417, 1961.
- Fejer, J. A., Theory of auroral electrojets, *J. Geophys. Res.*, 68,
2147-2157, 1963.
- Fukushima, N., *J. Fac. Sci. Tokyo Univ.*, 8, 293-412, 1953.
- Hones, E. W., Motions of charged particles trapped in the earth's
magnetosphere, *J. Geophys. Res.*, 68, 1209-1219, 1963.
- Kern, J. W., Solar stream distortion of the geomagnetic field and polar
electrojets, *J. Geophys. Res.*, 66, 1290-1292, 1961.

- Lyon, G. F. and A. Kavadas, Horizontal motions in radar echoes from aurora, 36, 1661-1671, 1958.
- Maeda, H., Horizontal wind systems in the ionospheric E region deduced from the dynamo theory of the geomagnetic Sq variations, Part 1. Non-rotating earth, J. Geomagnet. Geoelec., 7, 121-131, 1955.
- Maeda, H., Wind systems for the geomagnetic Sd field, J. Geomagnet. Geoelec., 9, 119-121, 1957.
- Martyn, D. F., Atmospheric tides in the ionosphere, I. Solar tides in the F₂ region, Proc. Roy. Soc. A., 189, 241-260, 1947.
- Matsushita, S., Ionospheric variations associated with geomagnetic disturbances, J. Geomagnet. Geoelec., 5, 109-135, 1953.
- Matsushita, S., Interrelations of sporadic E and ionospheric currents, in Ionospheric Sporadic E (Edited by E. K. Smith and S. Matsushita) Pergamon Press, 1962.
- Megill, L. R. and N. P. Carleton, Excitation by local electric fields in the aurora and the airglow, To be published, 1963.
- Obayashi, T. and J. A. Jacobs, Sudden commencements of magnetic storms and atmospheric dynamo action, Can. J. Phys., 62, 589-616, 1957.
- Silsbee, H. B. and E. H. Vestine, Geomagnetic bays, their frequency and current systems, Terr. Mag., 47, 195-208, 1942.
- Swift, D. W., The generation and effect of electrostatic fields during an auroral disturbance, J. Geophys. Res., 68, 2131-2140, 1963a.
- Swift, D. W., Electric fields and current flows in an auroral arc, AVCO Technical Report RAD-TR-63-14, April 1963b.
- Vestine, E. H., L. Laporte, I. Lange and W. E. Scott, The geomagnetic field - description and analysis, Carnegie Institute, Washington, 1947.

CAPTIONS FOR FIGURES

Figure 1. Schematic representation in the equatorial plane of the displaced belt of trapped protons and of a stream line of the low energy plasma rotating in the geomagnetic field distorted by the solar wind. The low energy plasma streams inward across the proton belt during the morning hours and outward during the evening hours.

Figure 2. The space charge, $|Q|$, of the trapped energetic protons contained in a tube of force that carves an area of 1 cm^2 (0.5 cm^2 at each of its feet) out of the ionospheric shell, as a function of the latitude. The solid and dashed curves were derived in I from the observations described by Davis and Williamson (1962), and represent two different extrapolations of their results. The triangular function indicated by solid lines represents the assumption of the present calculations.

Figure 3a-3d. The calculated amplitudes and phases of the height-integrated current density components as functions of the latitude, for different values of the height-integrated Hall conductivity $\int \sigma_2 dh$. The labels E and S denote the east and the south components of the height-integrated current density. The solid lines indicate the highest absolute value attained by each component during its diurnal variation; the interrupted lines show the local times when the sign of each component changes from positive to negative (east to west or south to north).

Figure 4a-4c. Lines of equipotential of the electric polarization field driving the currents of Fig. 3a-3d. The values of the height-integrated Hall conductivity $\int \sigma_2 dh$ and of the potential difference ΔV between neighboring lines are shown in each of the figures. The lines of equipotential can also be interpreted as lines of Hall current flow; the arrows indicate the direction of current flow.

Fig. 1

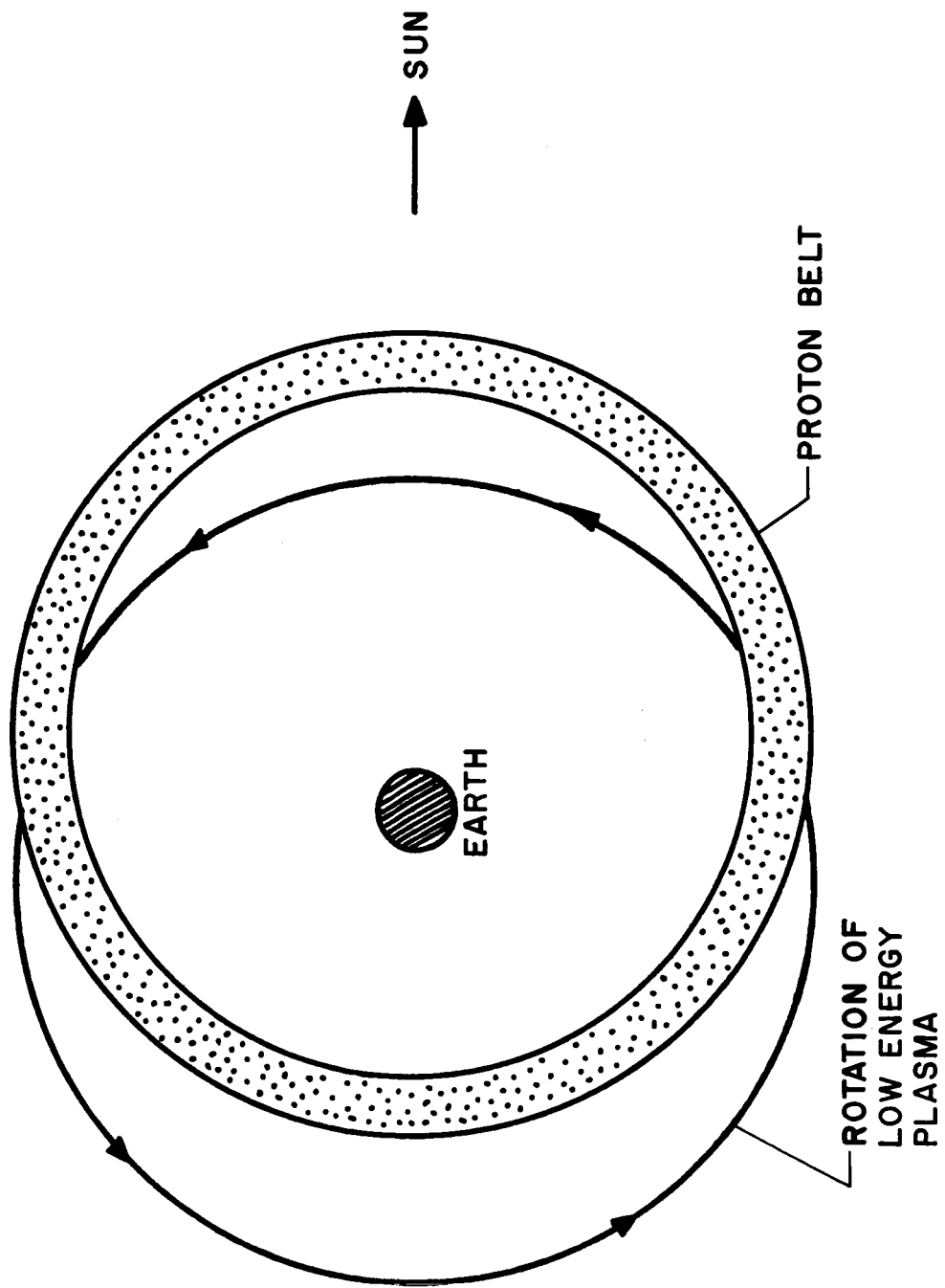


Fig. 2.

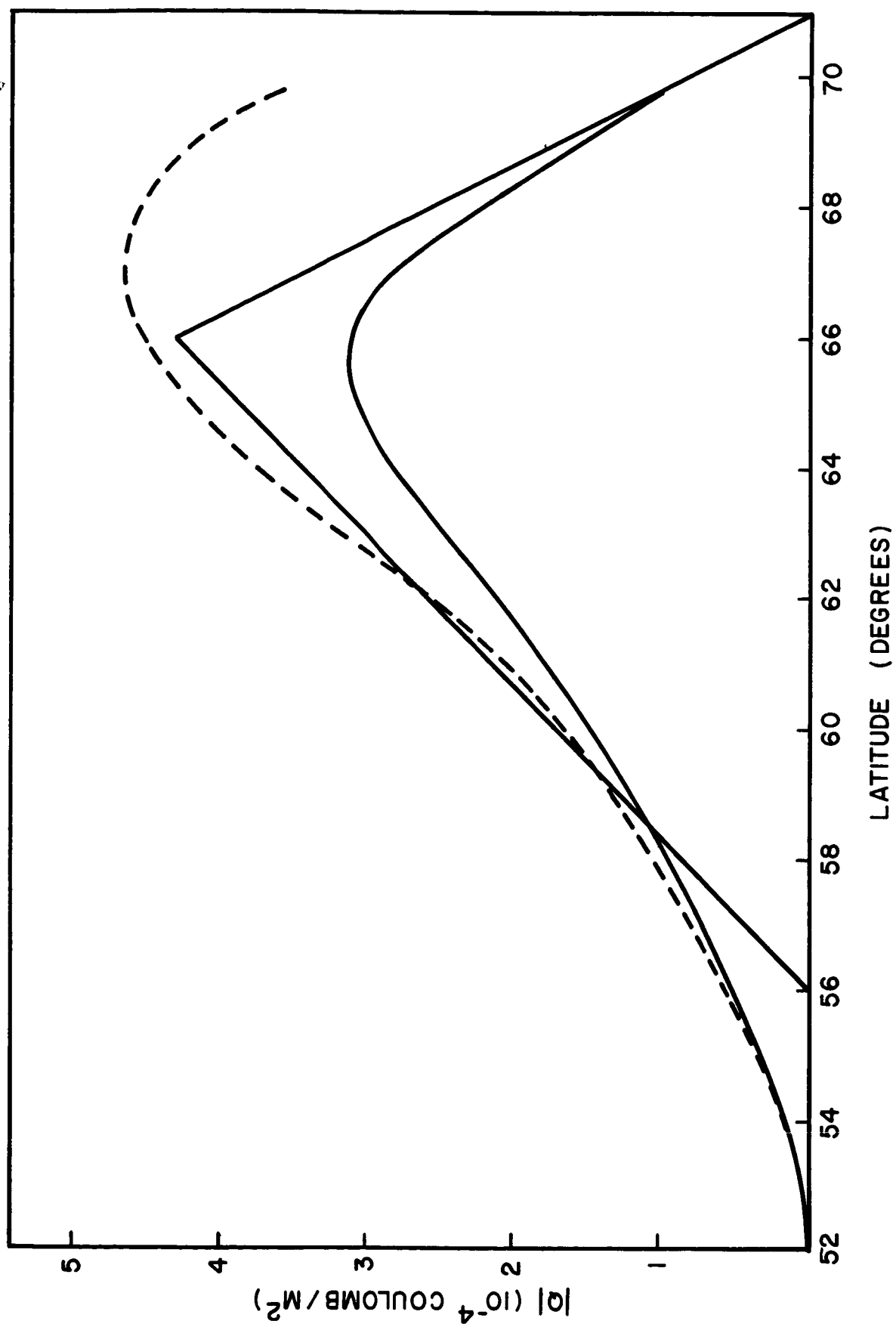


Fig 3a

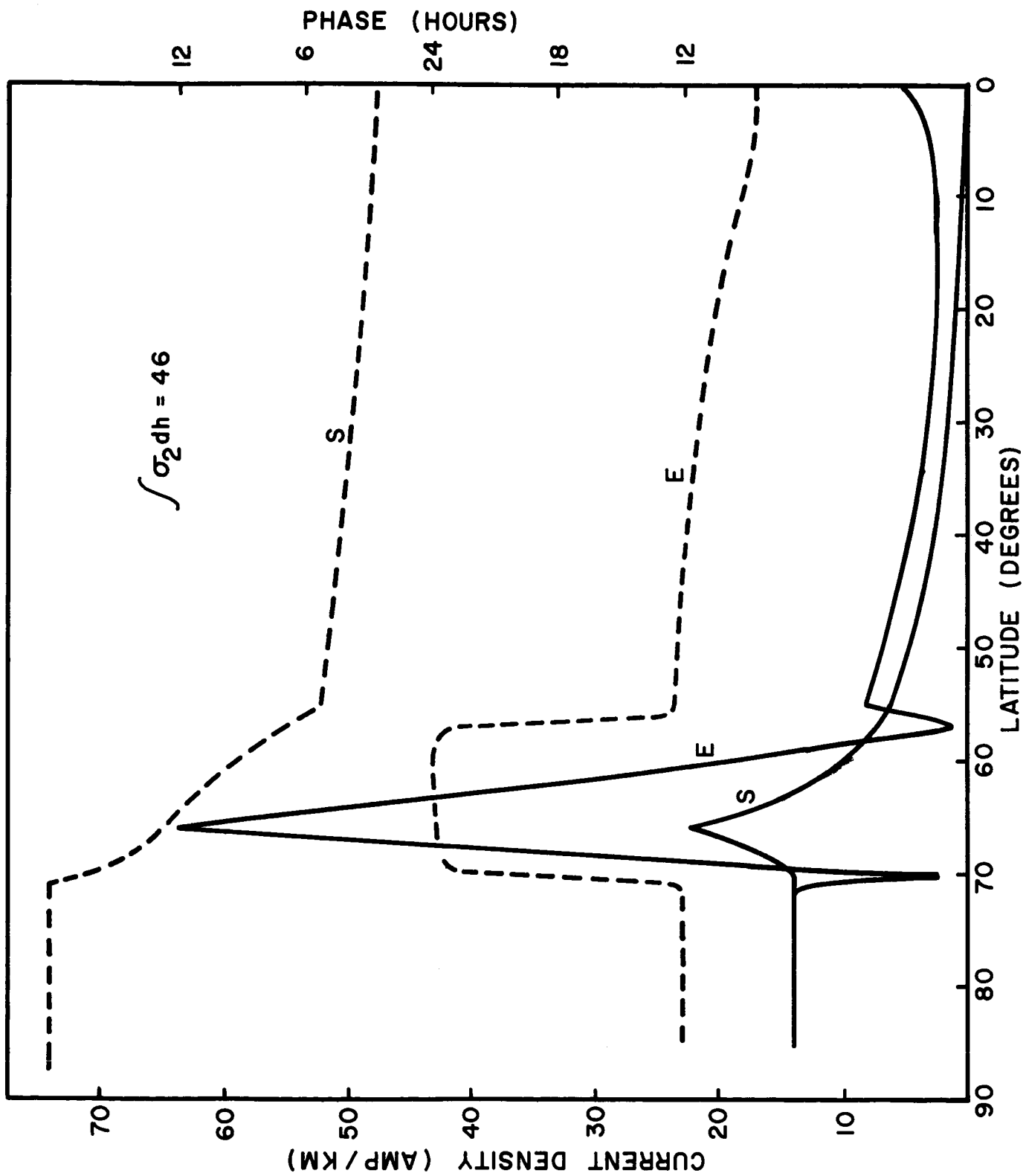


Fig 36

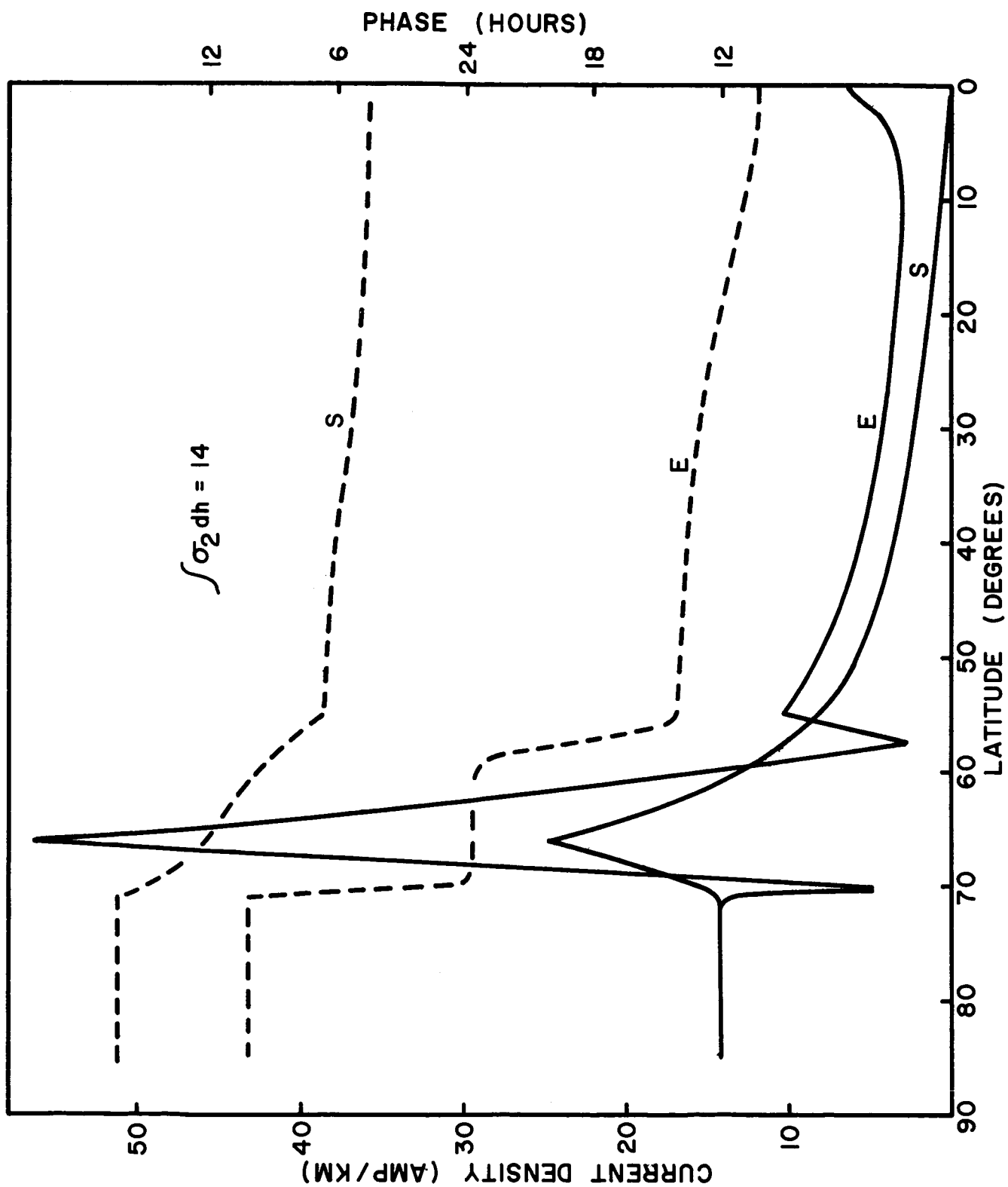


Fig. 3c.

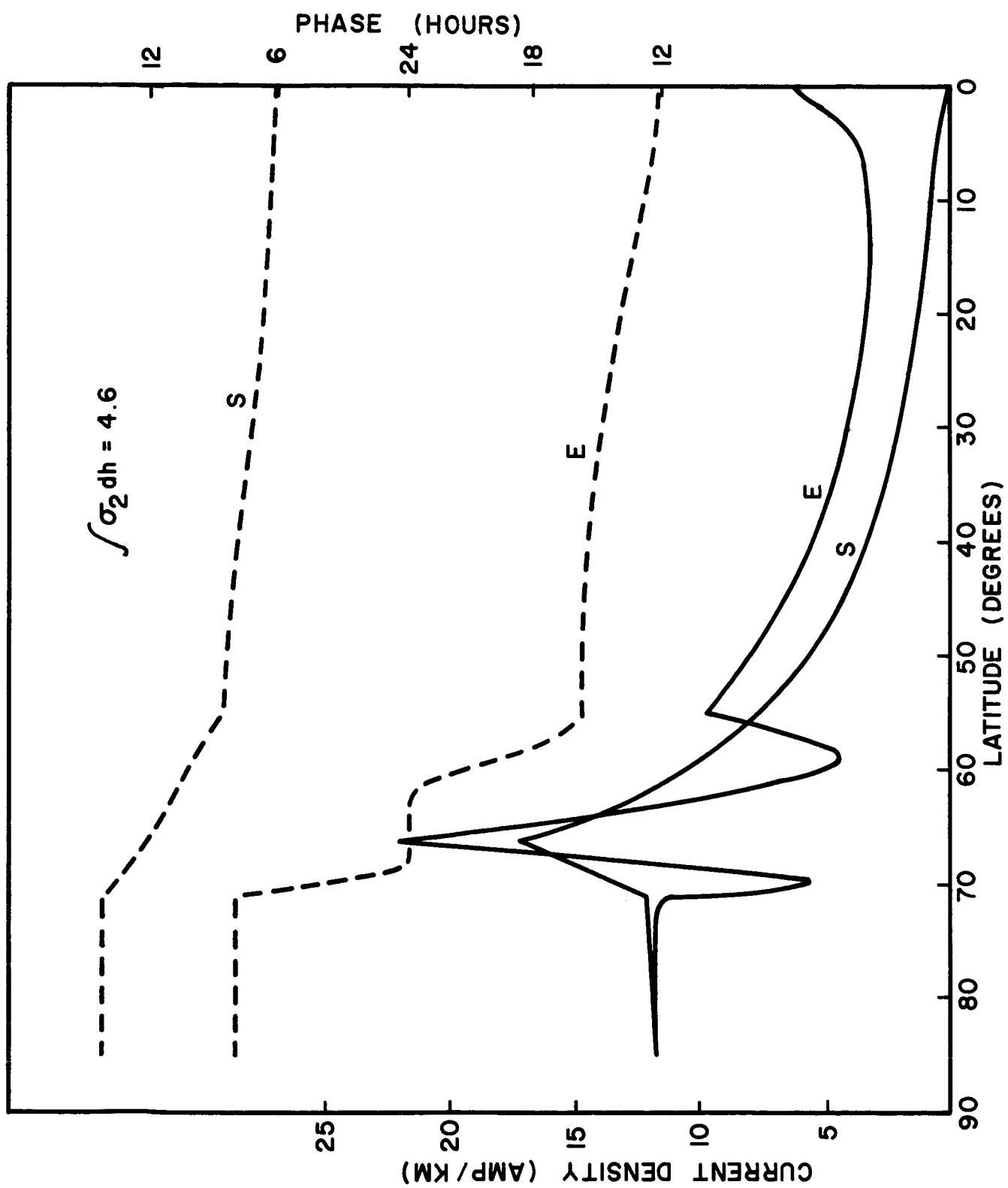


Fig 3d

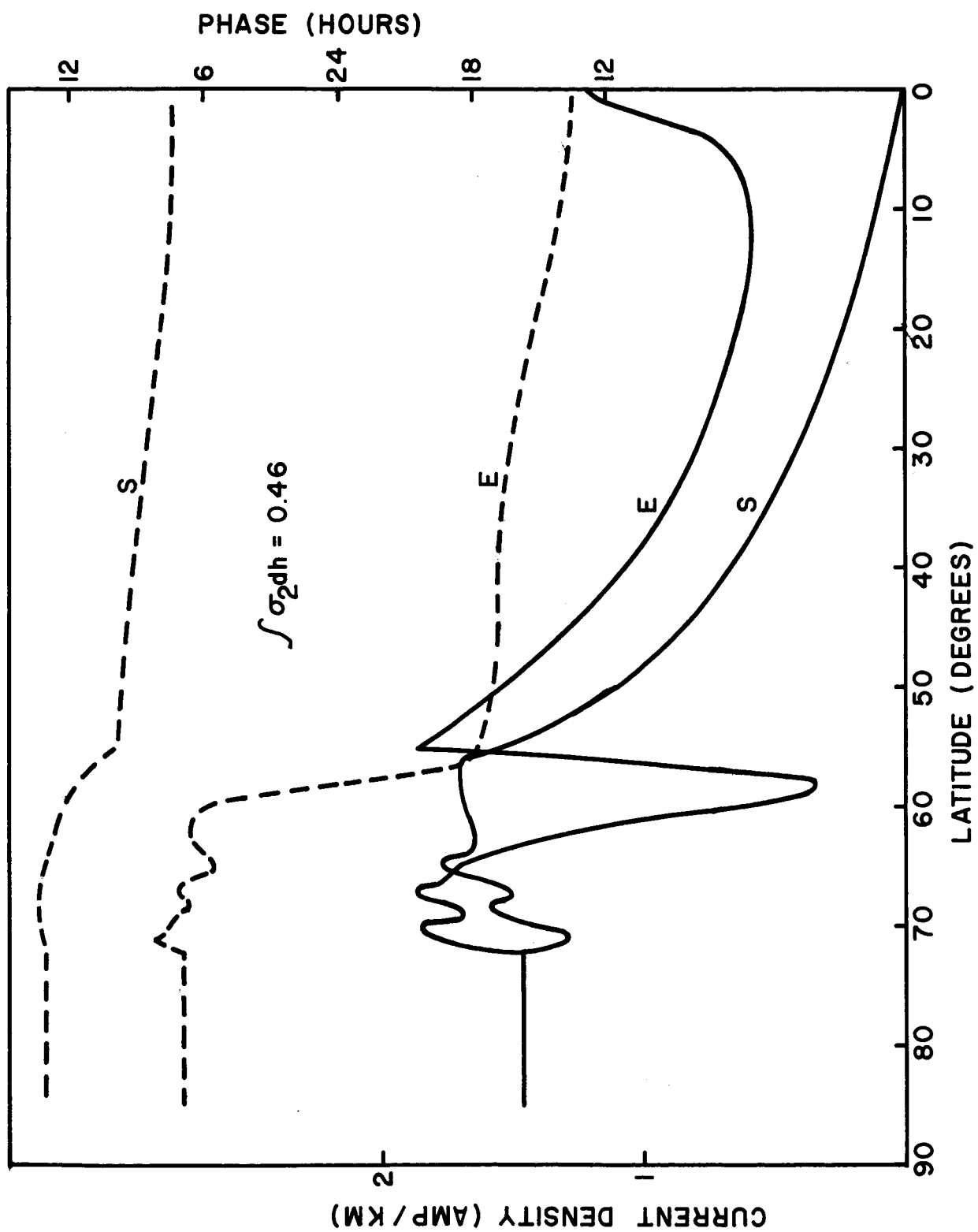
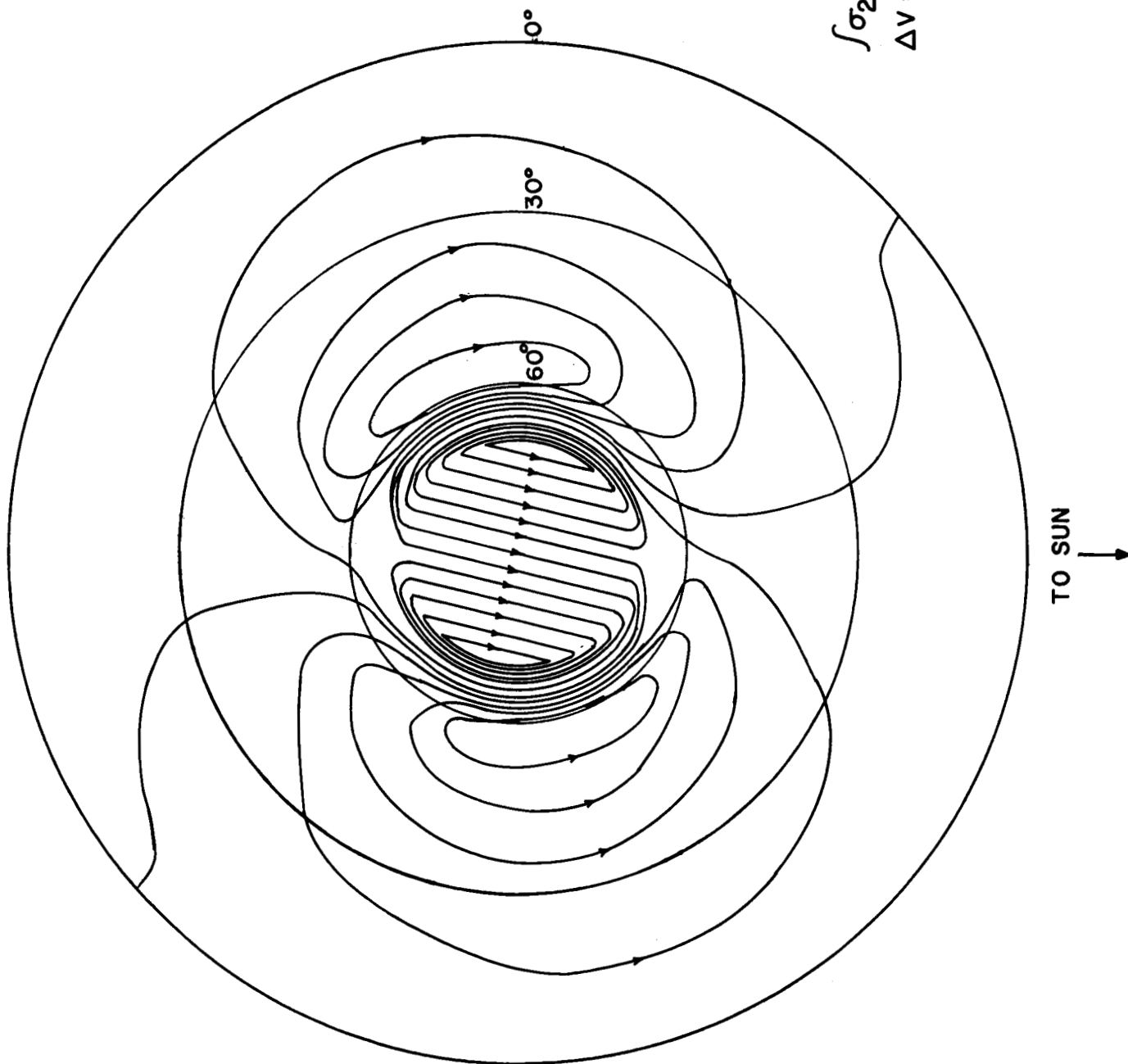


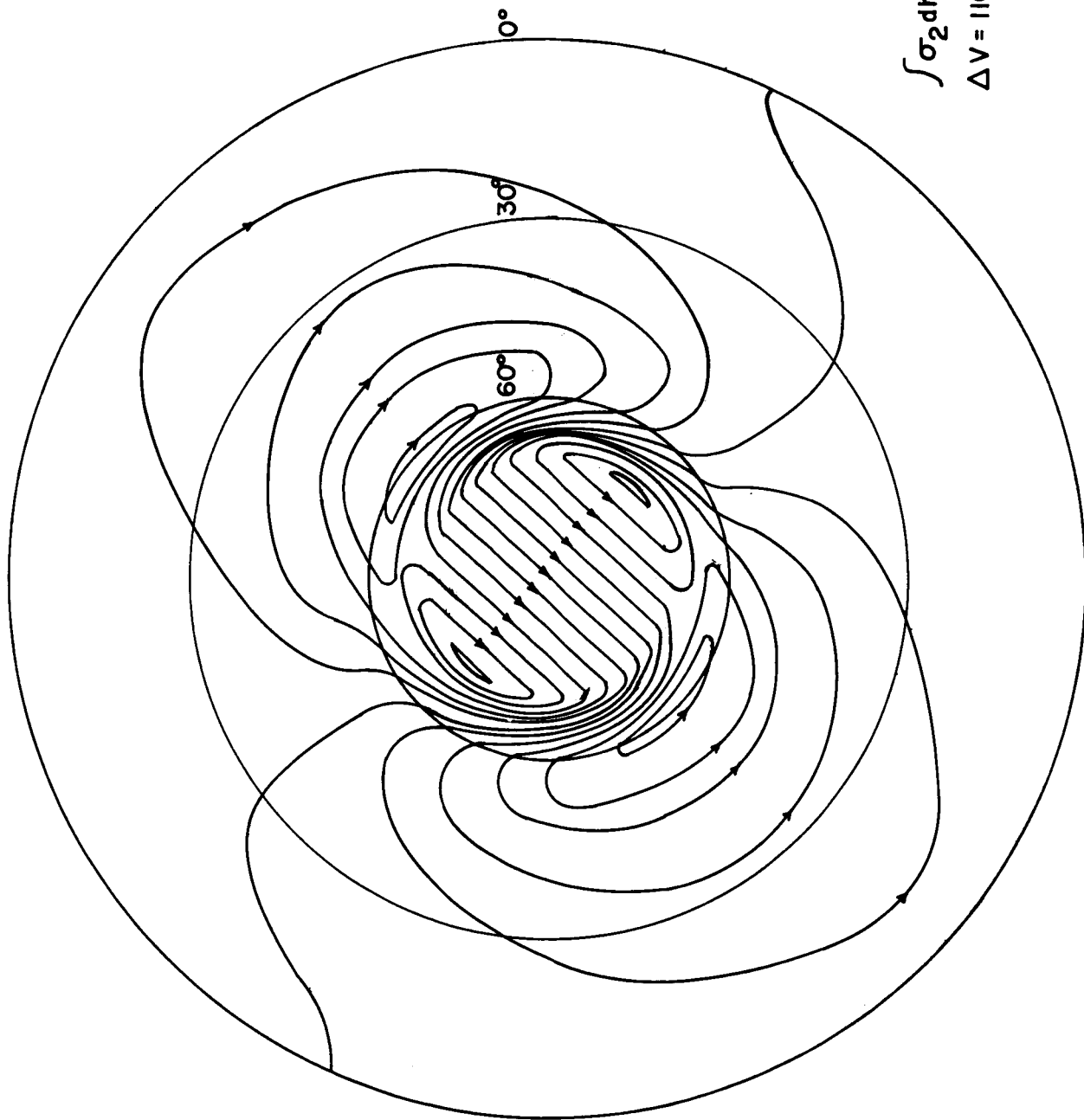
Fig. 4a.



$$\int \sigma_2 dh = 46$$

$$\Delta V = 290 \text{ VOLTS}$$

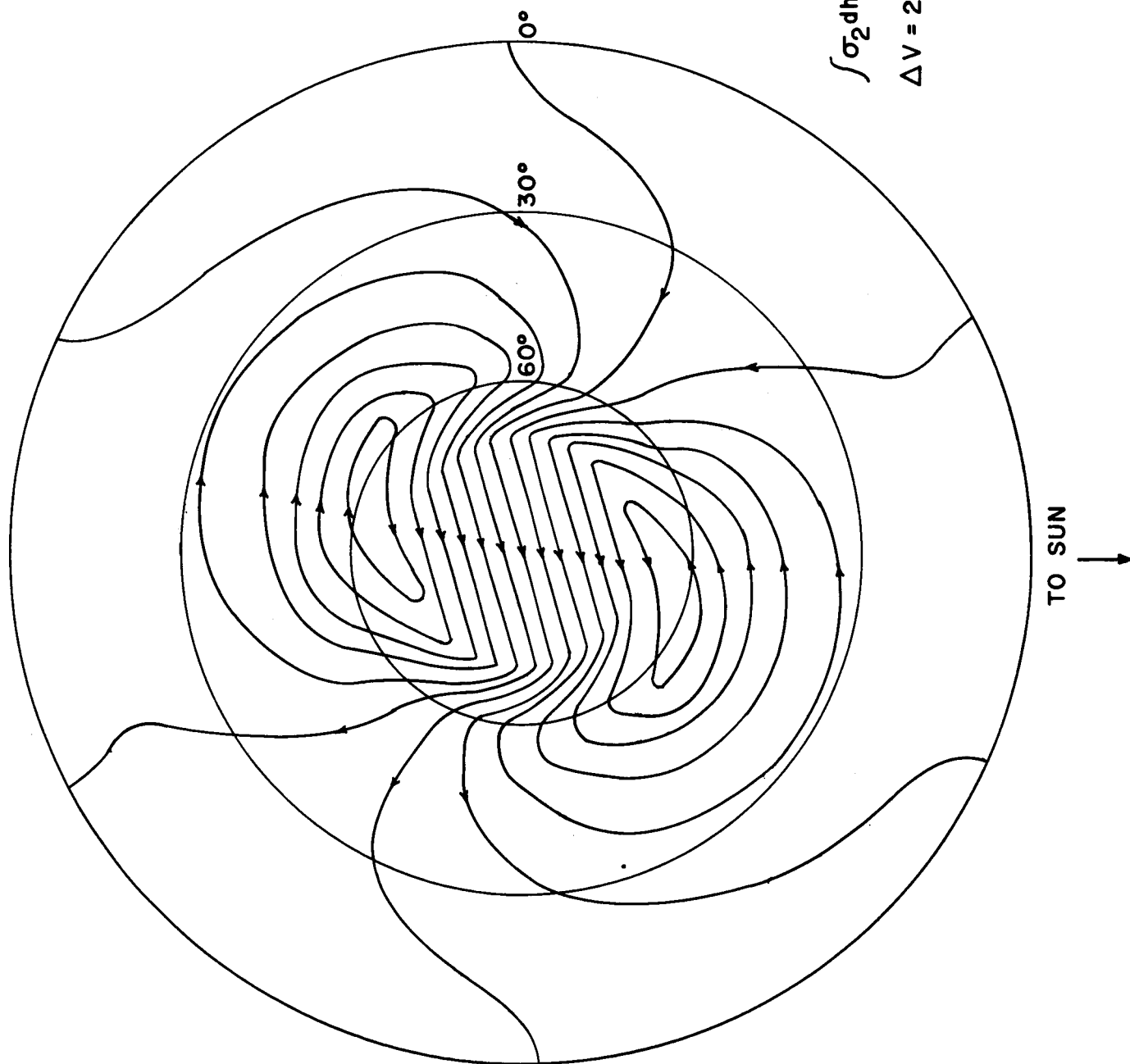
Fig 4b



$$\int \sigma_2 dh = 14$$
$$\Delta V = 1100 \text{ VOLTS}$$

TO SUN
↑

Fig. 4.



$$\int \sigma_2 dh = 4.6$$

$$\Delta V = 2900 \text{ VOLTS}$$